



Synthesized of Zinc-oxide Nanostructures by Sol-Gel Method

Abdul Quayoum

Department of Physics, A. Islamia Degree College, Lucknow

Email: abdulquayoum@gmail.com

Abstract

The present work is synthesis of ZnO nanostructures by sol-gel method. By X-ray diffraction (XRD) pattern structural study is performed and the formation of hexagonal phase is confirmed by XRD study. In photoconductivity study, we used to perform temporal response i.e. growth and decay of photocurrent. The photo-response of prepared sample has been measured under UV illumination using thick film of powder without any binder. The fast rise and decay of photocurrent has shown during the growth and decay of photocurrent indicating suitability for UV photo detectors.

Keywords: ZnO, Sol-gel, XRD, Photoconductivity.

1. INTRODUCTION

Due to their wide band gap (~3.37eV) and high exciton binding energy (~60 meV) at room temperature, Zinc-oxide (ZnO) Nanostructures have attracted tremendous interest for scientific community. It has been reported to display good photoconductivity and high transparency in the visible region and used as transparent electrodes for solar cells (Westernmark K. et. al., 2002).

Various methods have been used to synthesize ZnO nanostructures such as nanoparticles (NPs), nanorods (NRs) and nanowires (NWs) including chemical vapor deposition, sol-gel method, spray pyrolysis, co-precipitation method and hydrothermal method (Natsume Y. et.al.1992), Okamura T.et.al.,1992),(Aranovich J.et.al.,1979), (Kripal R.et.al.,2010), (Srivastava S.et.al., 2010),

In the present work, ZnO nanostructures have been prepared by thermal decomposition method. Owing to its simple, low-cost and mass-scale production, it is used at large scale.

In this work, optical emissions and photoconductivity properties of ZnO nanostructures have been investigated.

2. EXPERIMENTAL SECTIONS

2.1. *Sample preparation:* The zinc acetate dehydrate ($\text{Zn}(\text{CH}_3\text{COOH})_2 \cdot 2\text{H}_2\text{O}$) (99%, purity) from E. Merk Ltd. Mumbai, 400018, India was used as a precursor to prepare ZnO nanostructures. In this process, 2 gm of $\text{Zn}(\text{CH}_3\text{COOH})_2 \cdot 2\text{H}_2\text{O}$ was put into the crucible and calcined at 400 °C for 8 h in muffle furnace. Finally, we obtained ZnO nanostructures in powder form by thermal decomposition of zinc acetate dehydrate.

2.2. *Instrumentation:* The structural characterization of the prepared ZnO nanostructures was performed by X-ray diffraction (XRD), Rigaku D/MAX- 2200H/PC, CuK_α radiation. Photoluminescence (PL) was investigated by Perkin Elmer LS-55 fluorescence spectrometer. The photoconduction properties have been measured by inter-digitated cell type device (IDT) in photoconductivity measurements in which Cu electrodes etched on a Cu plate (PCB). The cell type device was used by putting a thick layer of powdered samples in between electrodes without any binder having a spacing of 1 mm. In this measurement, the direction of illumination was perpendicular to the field across the electrodes. The cell was mounted in a dark chamber with a slit where from the light is allowed to fall over the cell. The photo-response was measured by 300 W

UGC JOURNAL NO. 45204;

https://www.ugc.ac.in/journallist/ugc_admin_journal_report.aspx?eid=NDUyMDQ= IMPACT

FACTOR: 4.032 Page | 62

mercury light source. A dc field (50 V/cm to 500 V/cm) of constant stability was applied across the cell to which a dc nano-ammeter for the measurement of current and RISH Multi 18S with adapter RISH Multi SI 232 were connected in series.

3. RESULTS AND DISSCUSSION

3.1 Structural study

The X-ray diffraction (XRD) pattern of ZnO nanostructures synthesized by thermal decomposition method is shown in Figure 1.. X-ray diffraction pattern of ZnO nanoparticles exhibit that ZnO has hexagonal wurtzite structure and the peaks could be indexed according to standard JCPDS data (Zhang J.et.al., 2002). Furthermore, broadening in peaks implies that ZnO nanostructures have nanocrystalline nature. No other peak of impurities such as Zn(OH)₂ was observed.

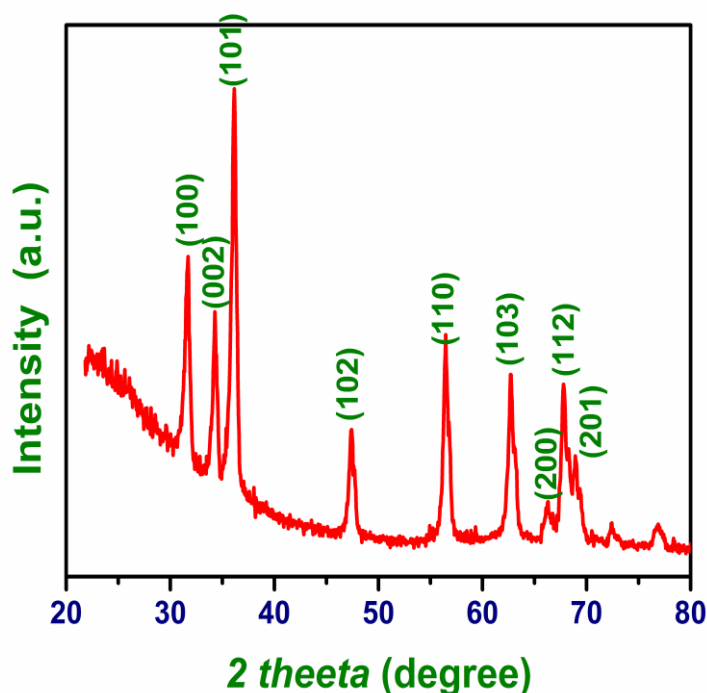


Figure 1: XRD pattern of ZnO nanostructures synthesized by thermal decomposition method.

3.2 Optical Properties

Photoluminescence study

Generally, visible optical emissions observed in ZnO is due to the intrinsic defects such as oxygen vacancies (V_o), zinc vacancies (V_{Zn}), oxygen interstitials (O_i), zinc interstitials (Zn_i) and oxygen antisites (O_{Zn}). Figure 2 shows photoluminescence spectrum of ZnO nanostructures synthesized by thermal decomposition method at excitation wavelength of 325 nm. In PL spectrum, several emission bands, including band edge emission at 385 nm, 394 nm and violet emission at 416 nm, blue emission at 443 nm, blue-green emission 483 nm and green emission 523 nm are observed. Band edge emission should be attributed to the recombination of excitons (Vanheusden K.et.al., 1996). The origin of violet emission centered at 2.96 eV (~ 416 nm) is ascribed to an electron transition from a shallow donor level of neutral Zn_i to the top level of the valence band (Fan X. M.et.al., 2005). A blue emission centered at ~2.56 eV (483 nm) is due to a radiative transition of an electron from the shallow donor level of Zn_i to an acceptor level of neutral V_{Zn} (Tatsumi T.et.al., 2004). Another blue emission was reported to appear at around 2.81 eV (443 nm) (Wang J.et.al., 2004). This emission may be related to surface defects of ZnO nanostructure or may be due to singly ionized V_{Zn}^- , although the detailed

mechanism for blue emission at 443 nm has not been clarified. The green emission 523 nm (~ 2.37 eV) are attributed to radiative transition from conduction band to the edge of the acceptor levels of O_{Zn} caused by oxygen antisites (O_{Zn}) (Murphy, T. E.et.al.,2006).

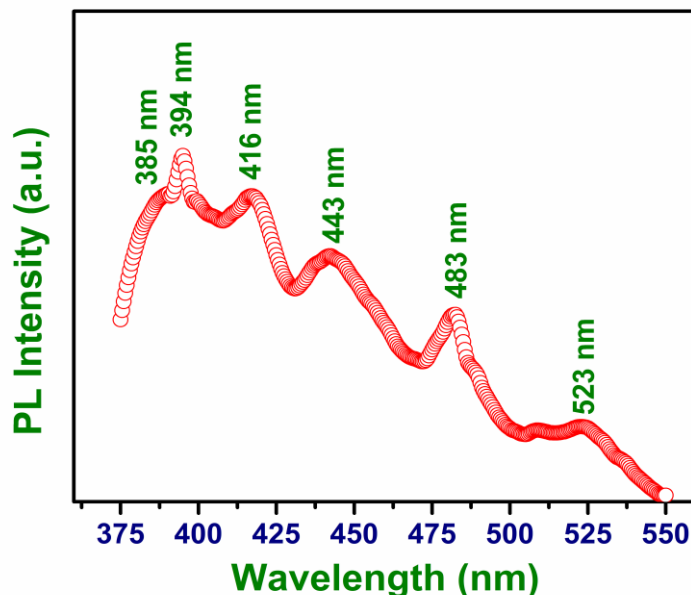


Figure 2: Photoluminescence spectrum of ZnO nanostructures synthesized by thermal decomposition method at 400 °C for 8h.

3.3 Photoconductivity study

Growth and decay of photocurrent

Generally, photoconduction properties in nanostructures are governed by two processes, the first one is surface related process and the second one is bulk-related process. In case of surface-related process, adsorption and desorption of chemisorbed oxygen takes place at the surface of materials because of large surface to volume ratio in nanocrystalline materials. In case of bulk-related process, photoconductivity is however considered to be faster than surface related process. In this process, oxygen molecules in the grain boundaries contribute to photoconductivity. Figure 3 shows growth and decay of photocurrent of ZnO nanostructures under illumination with fixed photo-flux and bias voltage (2500 lux, 20V). ZnO nanostructures demonstrate fast rise and decay of photocurrent under UV illumination. Naturally, ZnO nanostructures are n-type semiconductor because of oxygen vacancies and other native defects including interstitial Zn ions which act as donors in ZnO lattice. The fast growth and decay in photocurrent, due to the generation of photocarriers and their radiative and non-radiative recombination through local recombination centers present inside the materials (Bhat, S. V.et.al.,2009), (Blakesely J.C.et.al.,2008).

Trap depth determination

To calculate p -value (probability of an electron escaping from a trap) and trap-depth (E): The decay portion of photocurrent after the cessation of excitation has been taken. The plot for decay portion is well fitted by linear fitting of the photocurrent curve on a logarithmic scale. It is found that the decay portion can be governed by a single exponential law. The p -values corresponding to the exponential have been calculated by the relation (Bhat, S. V.et.al., 2009), (Blakesely J.C.et.al., 2008)

$$I = I_0 \exp(-pt)$$

Where I_0 is the current at the moment when light is interrupted and I is the photocurrent at any instant of time.

The theory of Randal and Wilkins for the emptying of traps assumes that the probability of an electron escaping from a trap is given by the equation:

$$p = S \exp (-E/kT)$$

where, the exponential term is a Boltzman factor involving the trap depth E , the absolute temperature T and Boltzman constant k (1.381×10^{-23} J/K); and S is the frequency factor i.e. the “attempt to escape frequency”. The attempt to escape frequency (S) may be interpreted as the number per second that the quanta from crystal vibrations (phonons) attempt to eject the electrons from the traps, multiplied by the probability of transition from trap to the conduction band, which is of the order of 10^9 at room temperature. The use of this equation requires the assumption that S and E are independent of temperature, and the electrons freed from traps are not re-trapped and the freed electrons undergo radiative, rather than dissipative transitions.

The trap depths (E) corresponding to different exponentials can be estimated by the expression:

$$E = kT \left[\log_e S - \log_e \frac{I_0}{I} \right]$$

The probability of an electron escaping from the trap and trap depths (trap ionization energies, eV) is 0.67 eV.

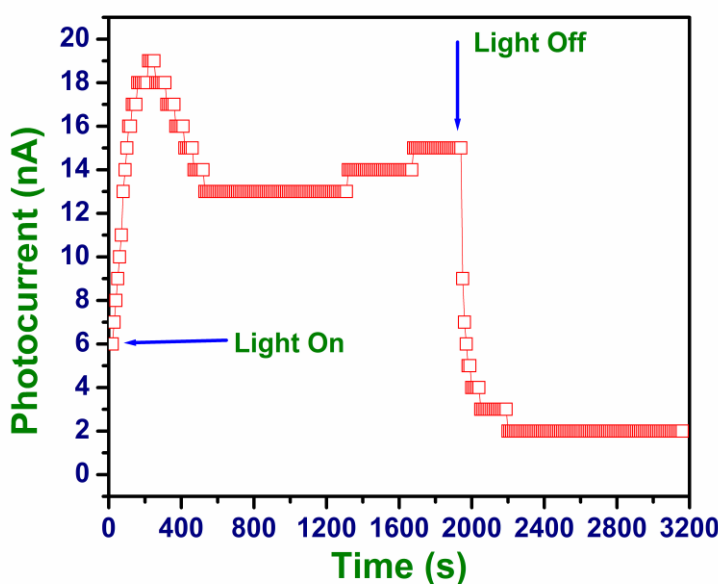


Figure 3: Growth and decay of photocurrent for ZnO nanostructures synthesized by thermal decomposition method at 400 °C for 8h under UV light illumination.

Spectral response of photocurrent

The spectral response i.e. the wavelength versus photocurrent spectrum of ZnO nanostructures synthesized by thermal decomposition method is shown in Fig. 4. Indicating clearly from Fig.4 that the photocurrent is maximum in lower wavelength region and it decreases for longer wavelengths. It can be inferred that the ZnO nanostructures are most photosensitive when excited by the incident light

near to the band gap energy which causes excitation of electron-hole pairs. The reduced photocurrent in visible range is due to excitation of localized defect states inside the band-gap that is also clearly seen in PL emissions in visible region (Srivastava S.et.al.,2010).

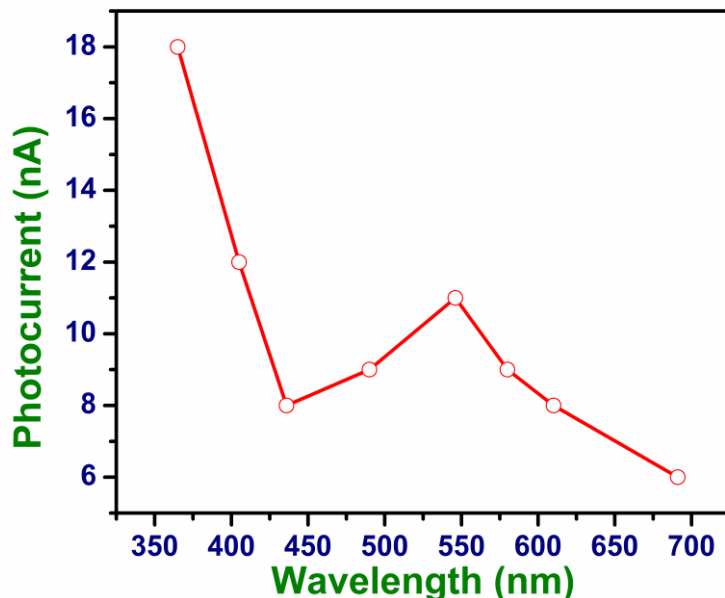


Figure 4: Spectral analysis of photocurrent for ZnO nanostructures synthesized by thermal decomposition method at 400 °C for 8h.

4. CONCLUSIONS

The Present investigation demonstrates photoluminescence and photoconductivity properties of ZnO nanostructures. XRD results of ZnO nanostructures exhibits hexagonal wurtzite structure. The photoluminescence spectrum exhibits broad visible emissions whereas photoconductivity shows fast growth and decay of photocurrent under UV illumination which is due to the fast generation and recombination of photocarriers. The trap depth is found to be 0.67 eV. The present work suggests promising applications in optoelectronics devices, such as switches, solar cells, photoconductor and sensors.

REFERENCES

1. Westernmark K.; Rensmo H.; Lees A. C.; Vos J. G.; and Siegbahn H. (2002) *Phys. Chem. B*, 106, 10108.
2. Natsume Y.; Sakata H.; Hirayama T.; and Yanagida H. (1992) *J. Appl. Phys.*, 72, 4203.
3. Okamura T.; Seki Y.; Nagakary S.; and Okushi H. (1992) *Jpn. J Appl. Phys*, 31, L762.
4. Aranovich J.; Ortiz A.; and Bube R. H. (1979) *J.Vac. Technol*, 16, 994.
5. Kripal R.; Gupta A. K.; Mishra S. K.; Srivastava R. K.; Pandey A. C.; Prakash S. G. *Spectr(2010) Acta Part:*
 - a. A, 76, 523.
6. Srivastava S.; Mishra S. K.; Yadav R. S.; Srivastava R. K.; Panday A. C.; Prakash S. G. *Digest J. of Nano.*
 - a. Bios. 2010, 5, 161.



7. Mishra S. K.; Srivastava R. K.; Prakash S. G.; Yadav R. S.; Pandey A. C.(2010) *Opto-Electron. Rev*, 18,
 - a. 467.
8. Zhang J.; Sun L. D.; Yin J. L.; Su H. L.; Liao C. S.; and Yan C. H.(2002) *Chem. Mater.* 14, 4172.
9. Vanheusden K.; Warren W. L.; Seager C. H.; Tallant D. R.; Voigt J. A.; Gnade B. E.(1996) *J. Appl. Phys.*
 - a. Vol. 79, 7983.
10. Fan X. M.; Lian J. S.; Zhao L.; Liu Y.(2005) *Appl. Surf. Sci.*, 252, 420.
11. Tatsumi T.; Fujita M.; Kawamoto N.; Sasajima M.; Horikoshi Y.(2004) *Jpn. J. Appl. Phys.* 43, 2602.
12. Wang J.; Gao L.(2004) *J.Cryst.Growth*, 262, 290.
13. Murphy, T. E.; Moazzami K.; and Phillips J. D.(2006) *J. Elect. Mater.* 35, 543.
14. Srivastava, R. K; and Prakash S. G.(2007) *Nat Acad Sci Lett*, 30, 11.
15. Smith, R. W.; and Rose, A(1955); *Phys. Rev.*, 97, 1531.
16. Bube, R. H.(1967) *Photoconductivity of Solids*, 404 John Wiley, New York.
17. Bhat, S. V.; Vivekchand, S. R. C.; Govindaraj, A.; Rao, C. N. R.(2009) *Solid State Commu*, 149, 510.
18. Jin Y.; Wang J.; Sun B.; Blakesely J.C.; and N.C. Greenham,(2008) *Nano Lett*, 8, 1649-1653.